J. Build. Mater. Struct. (2025) 12: 1-16 ***Original Article***
DOI : 10.34118/jbms.v12i1.4134

Mechanical Strength and Morphology of Spent Foundry Sand Containing Gum Arabic Concrete

Elinwa Augustine Uchechukwu

Civil Engineering Department, Abubakar Tafawa Balewa University, PMB 0248, Bauchi, Bauchi State, Nigeria.
Corresponding Author: *auelinwa@gmail.com*

Received: 30-01-2025 **Accepted: 07-05-2025**

Abstract. This work is on the experimental study of the effects of spent foundry sand (SFS) and gum Arabic (GA) on concrete properties using a concrete mix proportion of 1: 1.7: 2.6 and a cement content of 357 kg/m^3, water-cement (w/c) ratio of 0.5, and a GA dosage of 0.5 %. Six (6) levels of SFS replacements of 10 to 50 % were used and compared with the control concrete containing no SFS with and without 0.5 % GA. Analysis on the mechanical strength was performed using Minitab 18 Software. Also investigated were the hydration products using the XRD and SEM methods of analysis on the crushed concrete samples at the maximum strength (10 %). Some of the results of the investigation are that SFS and GA are compatible and can produce good quality concrete based on the statistical, XRD and SEM analysis. The dominant mineral oxides are CA, Si, Ag, Fe, C, K and Al with a very strong presence of Ca for concrete samples with both SFS and GA. These mineral oxides may have played substantial roles in the modification of the concrete samples.

Key words: Spent foundry sand, Gum Arabic, Compressive strength, Statistical analysis, XRD and SEM analysis.

1. Introduction

The sustainability of the construction industry is facing serious challenges from the acute shortage of conventional construction materials and their associated environmental impacts due to climate changes. The depletion of the earth's natural resources, accompanied by the greenhouse gases produced while processing these materials are of great concern. Actions to mitigate the effects of these challenges have been directed towards the use of waste materials and other supplementary cement materials (Olson, 2024). The excessive mining of high-quality river sand for cement sand mortar have been linked to environmental impacts and ecological imbalances (Akhtar, 2023). They also noted that replacing cement with silica fume helps reduce the environmental carbon footprint (Akhtar, 2023). The same concerns were expressed by Khuram Rashid and Sana Nazir who stressed that the conservation of natural resources, healthy environments, and optimal utilization of waste materials are intimate needs of the present time (Rashid and Nazir, 2018). Their work was both experimental and analytical using two types of used foundry sands to study the properties of concrete at replacement levels of 10 %, 20 % and 30 % (volume), and moist cured at 7, 28, and 63 days, to investigate the compressive strength along with the modulus of elasticity. Some of the results showed that there is a reduction in the compressive strength, but the modulus of elasticity increased as the amount of foundry sand was increased. Paul et al. (2021) have also highlighted the benefits of using spent chemical foundry sand (SCFS) through a case study conducted on the recovery of SCFS with an exhaustive physicochemical characterization of the by-product and analysis of its influence on workability and mechanical strengths of cementitious materials. The results of their investigations confirmed the suitability of the by-products. Also, the tests on workability and mechanical resistance on the mortars and concrete confirmed the influence of the fineness of the by-product associated with the parameters. Rafat

Siddique et al., (2009) presents the results of an experimental investigation carried as partial replacement of fine aggregate. This paper on the mechanical strength and characteristics of SFS-admixed concrete presents the results of an experimental investigation carried out to evaluate the mechanical properties of concrete mixtures in which fine aggregate (regular sand) was partially replaced with used-foundry sand (UFS). They replaced the fine aggregate with three percentages (10%, 20%, and 30%) of UFS by weight, and performed tests on the properties of fresh concrete. Compressive strength, splitting-tensile strength, flexural strength, and modulus of elasticity were determined at 28, 56, 91, and 365 days. Test results showed a marginal increase in the strength properties of plain concrete by the inclusion of UFS as partial replacement of fine aggregate. Experimental research studies on the effects of waste foundry sand (WFS) on the strength and microstructural properties of concrete have been investigated by Kumar et al. (2022), using tests on cubes, cylinders, and unreinforced beams, the mechanical properties of concrete made with waste foundry sand and manufactured sand as fine aggregate were assessed. Tensile, splitting, and flexural strengths of the concrete were all determined after 7, 14, 28, 56, and 90 days of curing. SEM, EDS, and Thermogravimetric Analysis (TGA/DCs) were also used to perform micro structural analyses on the control mixture and mixtures containing 10, 20, 30, 40, and 50% WFS. The strength differences that occur when fine aggregates are replaced with WFS in different proportions are better understood, thanks to the microstructural experiments. To justify its use as a replacement for fine aggregate in terms of strength and microstructure studies, just the right amount of WFS was added to the concrete.

The issue with sustainability in the construction industry is also concerned with the problems of the admixtures used for construction. These admixtures are mostly derived from conventional materials. For sustainability in the construction industry to be meaningful and impactful, recent research are directed in the areas of use of wastes and available local materials. These will complement their use as both supplementary cement materials (SCM) and admixture for concrete production. To optimize the use of SFS in concrete production GA was used as an emulsifier and an admixture. GA consists mainly of high-molecular weight polysaccharides with their calcium, magnesium, and potassium salts, which on hydrolysis, yield three main fractions of polysaccharides and proteins, including arabinogalactan (AG), arabinogalactan protein (AGP), and glycoprotein (GP) (Desplanques et al., 2012). Mohammed et al., (2018) used GA to improve the mechanical and physical properties of fresh and hardened concrete, and therefore, concluded it is a promising sustainable and environmentally friendly water-reducing admixture. Sugumaran and Neme (2024) investigated the influence of cement and Arabic gum on the physico-mechanical and microstructural properties of cementitious composites by varying quantities of Arabic gum on the hydration, fluidity, mechanical performance and microstructure of cement paste. They also investigated the influence of GA on slant shear performance and capillary water absorption. Some of their results indicated that the workability of cement was diminished because of the ability of GA to make the cement paste cohesive. Preliminary works on the use of GA with various combinations and mix have been carried out by the author, and same published as journal papers in various journals. Some of the works included: Using GA as an admixture for concrete production (Elinwa et al., 2018), XRD and microstructures studies of GA-cement concrete (Elinwa and Umar, 2017), mechanical strength of sawdust ash-admixed GA concrete (Elinwa, 2021), SFS-GA admixed concrete: XRD, microstructure, acid and sulphate analysis, and water absorption and density relations of GA-SDA concrete (Elinwa, 2024). Water absorption and density relations of GA-SDA concrete (Elinwa, 2022), and Density and mechanical strengths of GA-SDA concrete (Elinwa et al., 2021). The present work focused on the compressive strengths of SFS concrete at percentages of 10, 20, 30, and 40, by wt.% of fine aggregate. GA dosage of 0.5 % by wt.% of cement was added to the concrete and cured for 28 days in water and the results from the experimental works were subjected to statistical analysis to determine the effects of the additions (SFS and GA) on concrete, and the reliability of the experimental data. XRD and SEM methods of analysis were further used to study the hydration products of crushed cube compressive strength of the concrete samples at

10 and 20 % SFS replacements cured for 28 days. This was to study the effects of the additions on the concrete samples.

2. Materials Characteristics

2.1. Materials

Past works on SFS and its suitability for concrete has been raised because of grading surface properties and binder residues which needed to be assessed as they could make the SFS unsuitable for concrete (Mavroulidou and Lawrence, 2019). This issue of suitability of SFS and its use for concrete was extensively treated (Elinwa and Hazzard, 2017; Prasad et al., 2018; Elinwa, 2014). The physical and chemical properties of SFS and GA have also been significantly dealt with in accordance with the approved code of practices. They confirmed the compatibility of SFS and GA, and therefore suitable for good quality concrete. Spent foundry sand (SFS) was defined as a supplementary cementing material and the gum Arabic (GA) as an admixture in past works (Elinwa and Hazzard, 2017; Prasad et al.,2018; Elinwa, 2014). A summary of the physical and chemical properties of the SFS used overtime by past research in concrete is shown in Table 1a and Table 1b, respectively. Table 2 is the chemical properties of GA (Elinwa and Kabir, 2019; Elinwa, 2024).

Also established in past works are the XRDs and the morphologies of SFS and GA materials discussing in detail the crystalline phases, mineral oxides, and the structural characteristics of SFS and GA and their effects on the hydration products of the concrete samples. These are summarized as shown in Table 3 and Table 4.

Table 1a. Physical Properties of SFS.

Researcher	Physical Properties						
	S/Gravity	Absorption	F/Modulus	M/Content	≤ 75 μm	Unit Wt.	Clay & Others
Present Work	2.54	-	3.00	3.11		2589	-
Prasad et al., (2018)	2.40	1.70	1.86	Nil	-	-	-
Siddique et al., (2011)	2.61	1.30	1.78	-	18-00	1638	-
Ahmed et al., (2021)	2.34	4.08	3.33	-	-	1546	-
Bilal et al (2019)	2.55	1.48	1.90	-	-	1555	-
Guney et al., (2025)	2.45	-	-	3.25	24-00	-	-
Siddique et al., (2009)	2.20	1.30	1.60	-	8.00	1520	0.90
Raval et al., (2015)	2.49	0.43	-	0.1-9.80		2592	1.00 – 42.00
Elinwa (2014)	2.39	-	3.30	3.04	8.16	2589	-

3. Experiments on SFS-Gum Arabic Concrete

The aim of this experiment was to study the effects of SFS which is a supplementing cementing material (SCM) and GA an emulsifier and an admixture, on the mechanical strengths of concrete. Concrete mixtures with a mix proportion of 1: 1.7: 2.6, cement content of 357 kg/m^3, water-cement ratio of 0.5, and a GA dosage of 0.5 % were used to investigate the effects of SFS and GA on the water absorption, density and compressive strength. Six (6) levels of SFS replacements from 10 to 50 % were used and compared with the control containing no SFS with and without 0.5 % GA. The mixtures were labelled M-0, M-10, M-20, M-30, M-40, and M-50, respectively, the suffix indicating the level of replacement. The mixtures were proportioned for a target concrete cube strength of 25 kN/m^2 and a total of 90 cube specimen of size 100 mm was cast and cured for a period of 90 days.

Table 1b. Chemical Properties of SFS.

Oxide	Wt. (%)							
	Present	Paul et al., (2021)	Saddique et al., (2009)	Elinwa (2014)	Prasad et al., (2018)	Ahmad et al., (2021)	Bilal et al (2019)	Guney et al., (2010)
SiO_2	82.71	84.00	87.91	78.34	81.80	88.50	98.00	98.64
Al_2O_3	10.20	3.10	4.70	9.95	6.90	4.63	0.80	0.74
Fe_2O_3	3.92	3.60	0.94	2.14	2.30	0.83	0.25	1.01
CaO	0.98	0.30	0.14	2.64	3.55	0.90	0.035	0.35
MgO	0.15	0.70	0.30	0.41	0.32	0.21	0.023	0.50
SO_3	1.32	-	0.09	0.06	-	-	-	-
K_2O	0.06	0.40	0.25	1.14	0.90	0.01	0.04	0.21
Na_2O	0.29	-	0.19	0.15	0.60	0.02	0.04	1.07
P_2O_5	-	-	0.00	0.09	-	-	-	-
Mn_2O_3	-	-	0.02	0.05	-	-	-	-
TiO_2	-	0.10	0.15	0.78	-	-	-	-
$CaCO_3$	-	-	-	-	-	-	-	-
Cr_2O_3	-	4.60	-	-	-	-	-	-
NiO	-	0.30	-	-	-	-	-	-
As_2O_3	-	0.10	-	-	-	-	-	-
ZrO_2	-	0.10	-	-	-	-	-	-
SrO	-	-	0.03	-	-	-	-	-
LOI	0.93	1.60	5.15	2.47	-	-	-	-

Table 2. Chemical composition of GA

Oxide	Content	Detection limit	Error
SiO_2	8.3634	0.0000	0.0642
K_2O	0.7610	0.0000	0.0566
CaO	3.4673	0.0000	0.0666
MnO	0.0653	0.0000	0.0025
Fe_2O_3	0.2238	0.0000	0.0026
NiO	0.0331	0.0000	0.0011
SrO	0.0550	0.0000	0.0006
Y_2O_3	0.0027	0.0000	0.0000
Nb_2O_5	0.0539	0.0000	0.0003
MoO_3	0.2606	0.0000	0.0014
Ag_2O	0.0199	0.0000	0.0003
CdO	0.0903	0.0000	0.0019
HfO_2	0.0009	0.0000	0.0000

Table 3. Structural Weights - SFS

Element	Symbol	Atomic (%)	Weight (%)
Carbon	C	68.06	45.18
Silicon	Si	8.95	13.89
Iron	Fe	4.02	12.40
Oxygen	O	12.15	10.75
Aluminium	Al	4.96	7.40
Tantalum	Ta	0.54	5.42
Lead	Pb	0.25	2.86
Calcium	Ca	0.71	1.57
Magnesium	Mg	0.30	0.40
Titanium	Ti	0.05	0.14

Table 4. Structural Weights- GA

Element	At. Wt (%)	Wt. Conc (%)
C	68.18	59.61
O	22.02	25.64
B	5.60	4.40
Te	0.25	2.30
N	2.20	2.24
Ga	0.25	1.25
Ca	0.37	1.07
Br	0.14	0.83
As	0.11	0.60
K	0.16	0.46
Si	0.20	0.41
Rb	0.06	0.35
P	0.14	0.31
Mg	0.17	0.31
F	0.16	0.22

Table 5. Compressive Strengths of SFS and SFS-GA Concrete

Mix No	Age (days)					$^{7}/_{28}$ Strength
	3	7	28	60	90	
M-00	16.4	19.9	36.9	39.6	39.6	58.90
M-10-S	20.3	25.9	31.7	37.5	38.7	81.70
M-20-S	19.7	21.4	25.8	35.7	37.5	82.94
M-30-S	16.6	18.6	23.5	36.6	35.4	79.15
M-40-S	14.7	17.1	21.3	34.7	35.4	80.28
M-50-S	7.7	8.1	12.1	14.6	15.1	95.06
M-00-SG	17.4	24.7	31.3	33.0	38.4	78.91
M-10-SG	18.7	19.4	26.0	32.6	34.8	74.62
M-20-SG	18.0	19.4	25.7	29.8	31.9	75.49
M-30-SG	17.7	18.8	20.6	24.6	31.3	91.26
M-40-SG	15.7	16.8	19.9	28.7	29.5	84.42
M-50-SG	7.0	7.5	13.3	13.9	14.1	56.39

Table 6: Compressive Strength Difference for SFS and SFS-GA Concrete

Age	M-00	M-10	M-20	M-30	M-40	M-50
	Percentage Difference (%): $^{M_2 - M_1}/_{M_1}$ x 100 %					
3d	6.10	14.02	9.76	7.93	-4.27	-57.32
7d	24.12	-2.51	-2.51	-5.53	-15.58	-62.31
28d	-15.18	-29.54	-30.35	-44.17	-46.07	-63.96
60d	-16.67	-17.68	-24.75	-37.88	-27.53	-64.89

Three (3) cubes were tested to failure at the end of every curing regime, and the average recorded. The study established the reliability of the results of the data on the cube compressive strengths using statistical characteristics such as the mean and standard deviation. Again, standard acceptance tests were also carried out on the two indicators, *the Mix* and *the Age*, to assess the mechanical properties of the concrete samples by examining if a production lot of the concrete was fulfilling the design requirements or not. Tables 5 is the cube compressive strengths, and the 7-28th day strengths results for the concrete samples, while Table 6 is the strength difference in percentage.

The statistical values of the concrete samples were conducted on the data from the experimental results on the two parameters, the characteristics indicators are the *Mix* and *the Age,* using the statistical packages in the Minitab 18 Software. The results of such analysis are shown in Table 7, Table 8, Table 9 and Table 10, for SDA-concrete samples, and SDA-GA concrete respectively.

Table 7: Descriptive Statistics: Compressive Strength for SDA-Concrete [Age]

Age	Mean	SE Mean	StDev	Variance	CoefVar
3d	15.90	1.85	4.54	20.64	28.58
7d	18.50	2.42	5.92	35.05	32.00
28d	25.22	3.51	8.59	73.84	34.08
60d	33.12	3.77	9.22	85.09	27.85
90d	33.62	3.77	9.23	85.19	27.46

Table 8: Descriptive Statistics: Compressive Strength for SDA-Concrete: [Mix]

Mix	Mean	SE Mean	StDev	Variance	CoefVar
-M-00	29.72	2.96	9.35	87.36	31.45
M-10	28.56	2.38	7.53	56.76	26.38
M-20	26.49	2.22	7.01	49.08	26.45
M-30	24.37	2.37	7.48	55.94	30.69
M-40	23.38	2.52	7.97	63.54	34.09
M-50	11.34	1.06	3.34	11.19	29.49

Table 9: Descriptive Statistics: Compressive Strength for SDA-GA Concrete [Age]

Age	Mean	SE Mean	StDev	Variance	CoefVar
3d	15.75	1.80	4.40	19.37	27.94
7d	17.77	2.32	5.67	32.16	31.92
28d	22.80	2.55	6.24	38.88	27.35
60d	27.10	2.92	7.15	51.08	26.37
90d	30.00	3.43	8.39	70.39	27.97

Table 10: Descriptive Statistics: Compressive Strength for SDA-GA Concrete [Mix]

Mix	Mean	SE Mean	StDev	Variance	CoefVar
M-00	28.96	3.62	8.10	65.67	27.98
M-10	26.30	3.30	7.37	54.35	28.03
M-20	24.96	2.75	6.15	37.87	24.66
M-30	22.60	2.47	5.53	30.54	24.45
M-40	22.12	2.93	6.56	43.05	29.66
M-50	11.16	1.60	3.59	12.86	32.13

3.1. Hydration Characteristics of the Concrete Samples

The characteristics of the hydration products of the concrete samples were studied using crushed samples of the cube compressive strengths at 10 % and 20 % fine aggregate replacements. The details of the XRD diffractograms on the crystalline peaks (height) and mineral phases were extensively discussed in the previous publications (Elinwa, 2024). The study here, therefore, are extrapolation on the data from that study. The results are used to evaluate the effects of the two additions (SFS and GA) on *the Mix* and *the Age* performances of the concrete samples. The performance characteristics (QA) for these concrete samples are shown in Table 11, Table 12, and Table 13, respectively. Table 11 shows the crystalline phases and peak heights. Table 12 and Table 13 are *the Age* and *the Mix* performances of the concrete samples.

Table 11: Crystalline Phases and Peak Heights (Elinwa, 2024)

Repl (%)	SFS-Concrete			SFS-GA Concrete		
	Position	Crystal line Phase No	Peak Height @ 100 % Intensity	Position	Crystalli ne Phase No	Peak Height @ 100 % R.Intensity.
00	20.0892-68.1389	10	218.00	26.856-68.1389	6	89.55
10	20.0892-68.1389	10	210.21	26.7624-8.6905	7	131.33
20	20.0892-68.1389	10	204.20	5.7294-53.63.6374	6	65.47

Table 12: Characteristics and Comparison of the Mineral Oxides -Age of Concrete

Repl. (%)	*Mineral Name*	*Formula*	Quantity (%)		Performance Characteristics Diff (%)
			Control	*10 % SFS Concrete*	
Control Plus10% SFS	Hildebrandt	$Ca_3 H_2 O_{7.5} Si_{1.5}$	51.2	52.2	1.95
	Quartz	SiO_2	21..0	15.2	- 27.62
	Brownmillerite	$Al Ca_2 Fe O_5$	12.0	14.7	22.50
	Portlandite	$Ca H_2 O_2$	8.9	9.2	3.37
	Tricalcium aluminate	$Al_2 Ca_3 O_6$	6.9	8.7	26.09
Control Plus20% SFS	*Mineral Name*	*Formula*	*Control*	*20 % SFS*	*Diff. (%)*
	Hildebrandt	$Ca_3 H_2 O_{7.5} Si_{1.5}$	51.2	36.8	- 28.13
	Quartz	SiO_2	21..0	21.6	2.86
	Brownmillerite	$Al Ca_2 Fe O_5$	12.0	20.9	74.17
	Portlandite	$Ca H_2 O_2$	8.9	16.0	79.78
	Tricalcium aluminate	$Al_2 Ca_3 O_6$	6.9	4.7	- 31.88
!0 % SFS and 20 % SFS Concrete	*Mineral Name*	*Formula*	*10 % SFS*	*20 % SFS*	*Diff. (%)*
	C	$Ca_3 H_2 O_{7.5} Si_{1.5}$	52.2	36.8	- 29.50
	Quartz	SiO_2	15.2	21.6	42.11
	Brownmillerite	$Al Ca_2 Fe O_5$	14.7	20.9	42.18
	Portlandite	$Ca H_2 O_2$	9.2	16.0	73.91
	Tricalcium aluminate	$Al_2 Ca_3 O_6$	8.7	4.7	- 45.98
10 % SFS-GA and 20 % SFS-GA	*Mineral Name*	*Formula*	*10 % SFS-GA*	*20 % SFS-GA*	*Diff. (%)*
	Hildebrandt	$Ca_3 H_2 O_{7.5} Si_{1.5}$	51.5	36.8	- 28.54
	Quartz	SiO_2	17.8	21.6	21.35
	Brownmillerite	$Al Ca_2 Fe O_5$	13.7	20.9	52.55
	Portlandite	$Ca H_2 O_2$	8.9	16.0	79.78
	Tricalcium aluminate	$Al_2 Ca_3 O_6$	8.1	4.7	- 41.98

Table 13: Characteristics and Comparison of Mineral Oxide Difference (%) – Mix of the Concrete

Repl. (%)	Mineral	Formula	SFS Concrete	SFS-GA Concrete	Performance Diff (%)
10	Hildebrandt	$Ca_3 H_2 O_{7.5} Si_{1.5}$	52.2	51.5	-1.34
20	Hildebrandt	$Ca_3 H_2 O_{7.5} Si_{1.5}$	34.4	36.8	6.98
10	Quartz	SiO_2	15.2	17.8	17.11
20	Quartz	SiO_2	32.4	21.6	-33.33
10	Brownmillerite	$Al Ca_2 Fe O_5$	14.7	13.7	-6.80
20	Brownmillerite	$Al Ca_2 Fe O_5$	16.7	20.9	25.15
10	Portlandite	$Ca H_2 O_2$	9.2	8.9	-3.26
20	Portlandite	$Ca H_2 O_2$	13.5	16.0	18.52
10	Tricalcium aluminate	$Al_2 Ca_3 O_6$	8.7	8.1	-6.90
20	Tricalcium aluminate	$Al_2 Ca_3 O_6$	3.0	4.7	15.75

3.2. Microstructure of SFS and SFS-GA Modified Concrete

Figure 1, Figure 2 and Figure 3 showed the morphology of the concrete samples compared with the control concrete. The derivations again were based on the hydration products derived from the crushed cube compressive strength. The structural characteristics (EDS) showing the atomic and weight concentrations (%) of the oxides of the hydration products are shown in Table14 for *the Age* of the concrete samples and Table 15, *the Mix* of the concrete samples.

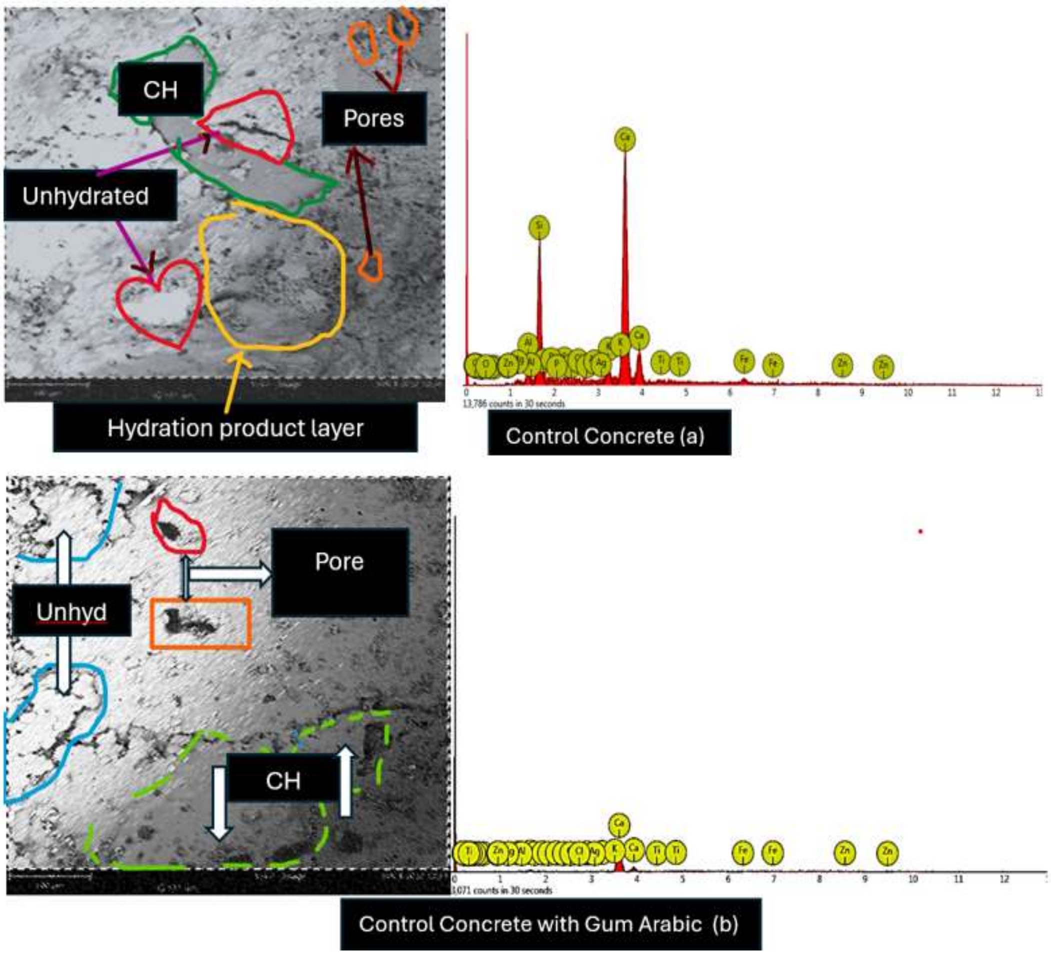

Fig. 1: Micrograph and EDS Spectrum - Control Concrete (a): Control-GA Concrete (b)

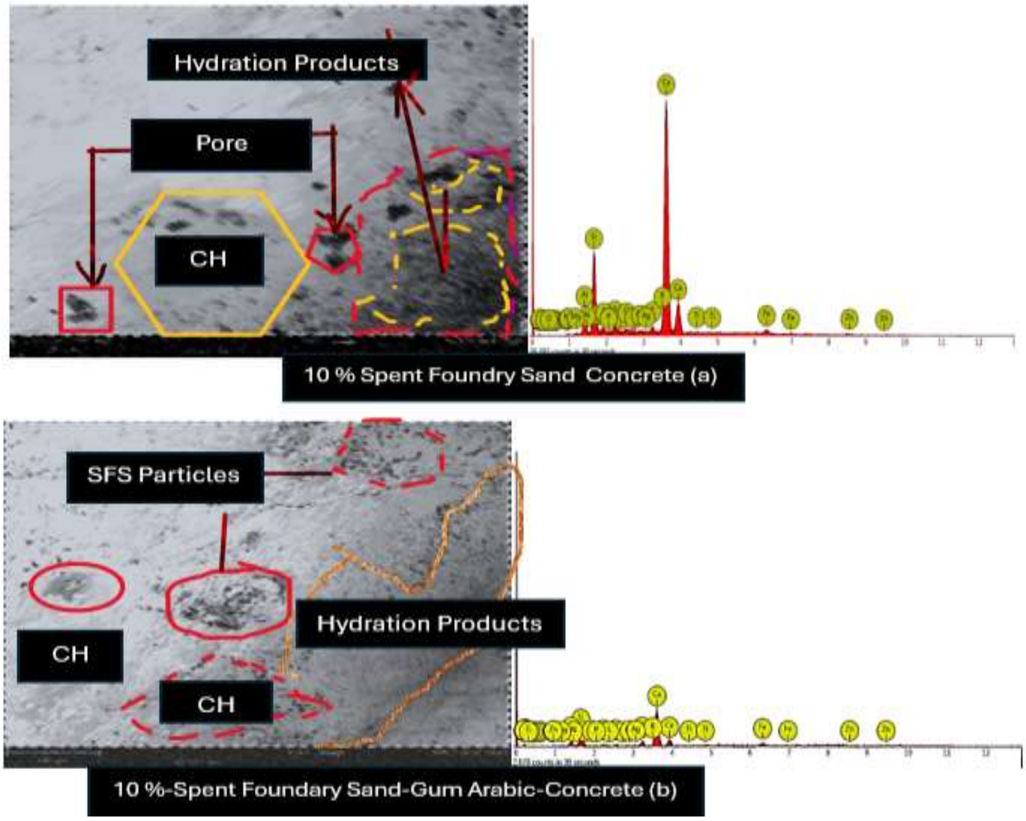

Fig. 2: Micrograph and EDS Spectrum -10 % SFS-GA Concrete

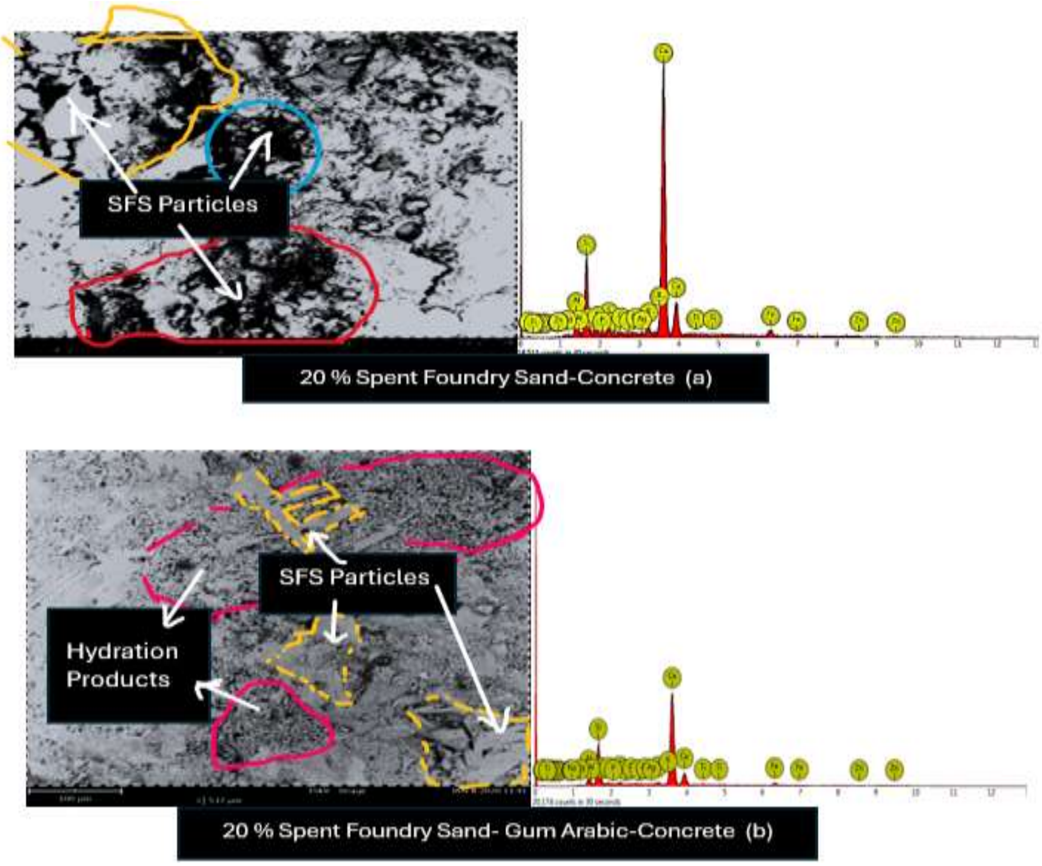

Fig. 3: Micrograph and EDS Spectrum of 20 % SFS-GA Concrete

Table 14: Characteristics of the Concrete Samples – Age of Concrete Samples

S/No	Oxide	Symbol	Repl. %			% Diff		
			0	10	20	0-10	0-20	10-20
Addition- Spent Foundry Sand (SFS)								
1	Calcium	Ca	61.38	68.77	64.62	12.04	5.28	- 6.03
2	Silver	Ag	17.24	2.80	2.66	- 83.76	- 84.57	- 5.00
3	Iron	Fe	4.38	3.14	6.23	- 28.31	42.24	98.41
4	Carbon	C	3.63	1.09	1.38	-69.97	-61.98	26.61
5	Potassium	K	3.07	1.53	1.75	-50,16	- 43.00	14.38
6	Silicon	Si	17.24	11.38	13.82	-33.99	- 19.84	21.44
7	Potassium	P	1.71	1.04	1.04	-39.18	-39.18	0.00
8	Aluminium	Al	1.30	3.57	3.61	174.62	177.69	1.12
9	Sodium	Na	1.18	0.31	0.17	-73.73	- 85.59	-45.16
10	Sulphur	S	1.04	1.41	1.52	35.58	46.15	7.80
11	Magnesium	Mg	0.88	0.23	0.34	- 73.86	- 61.36	47.83
12	Chlorine	Cl	0.68	1.09	0.76	60.29	11.76	- 30.28
13	Oxygen	O	0.40	0.58	0.15	45.00	- 6.25	-74.14
14	Titanium	Ti	0.14	0.22	0.00	57.14	-100	-100
15	Zinc	Zn	0.00	2.84	1.95	100	100	-31.34-
Addition-Spent Foundry Sand-Gum Arabic (SFS-GA)								
1	Calcium	Ca	80.90	54.74	64.62	- 14.99	- 20.12	- 6.03
2	Silver	Ag	3.90	2.80	2.66	- 28.21	- 31.79	- 5.00
3	Iron	Fe	3.07	11.89	6.23	2.28	102.93	98.41
4	Carbon	C	2.63	1.09	1.38	-58.56	- 47.53	26.61
5	Potassium	K	2.27	1.53	1.75	- 32.60	-22.91	14.38
6	Silicon	Si	2.17	9.27	13.82	424.42	536.87	21.44
7	Potassium	P	1.18	1.04	1.04	- 11.86	-11.86	0.00
8	Aluminium	Al	1.08	3.68	3.61	230.56	234.26	1.12
9	Sodium	Na	0.91	0.31	0.17	- 65.93	- 81.32	- 45.16
10	Sulphur	S	0.87	1.41	1.52	62.07	74.71	7.80
11	Magnesium	Mg	0.55	0.23	0.34	- 58.18	-38.18	47.83
12	Chlorine	Cl	0.46	1.09	0.76	136.96	65.22	- 30.28
13	Oxygen	O	0.00	0.58	0.15	100.00	100.00	- 74.14
14	Titanium	Ti	0.00	0.22	0.00	100.00	0.00	-100.00
15	Zinc	Zn	0.00	2.84	1.95	100.00	100.00	- 31.34

4. Discussions

4.1. Characteristics of the Materials

4.1.1. Physical and Chemical Properties

Tables 1 (a and b), 2, and 3 showed that the characteristics of spent foundry sand (SFS) and gum Arabic (GA). Earlier studies on concrete materials showed the total oxides in cement, SFS, and GA are 29.4 %, 96.83 %, and 8.36 %, respectively. SFS has high affinity for water because of its texture occupying more surface area with ultra-fineness (Elinwa, 2014). The specific gravity of fine aggregate has been identified as a relevant parameter in the formulation of concrete that has influenced their volume proportion in the cementitious materials as well as the density of the latter. GA on the other hand, has been confirmed to improve workability and compressive strength (Saleh, 2001; Mbugua et al., 2016) and can reduce water to cement ratio (w/c) from 0.61 to 0.48 (Siddique et al., 2010). Studies on the physical and chemical properties of SFS showed variability which are tied to some factors like the environment and conditions of use (Paul et al., 2021). The characteristics of both the SFS and GA influenced the final hydration products of the concrete samples.

Table 15: Structural Characteristics of SFS-GA Concrete -Mix of the Concrete Samples

Element Oxide	Symbol	Weight (%)		Diff. (%)	Remarks
		Without GA	*With GA*		
Control Concrete (0 %) Replacement					
Calcium	Ca	61.38	80.90	24.13	Increase
Silver	Ag	17.24	3.90	-342.05	Decrease
Iron	Fe	4.38	3.07	-42.67	Decrease
Carbon	C	3.63	2.63	-38.02	Decrease
Potassium	K	3.07	2.27	-35.24	Decrease
Silicon	Si	2.98	2.17	-37.33	Decrease
Phosphorus	P	1.71	1.18	-44.92	Decrease
Aluminium	Al	1.30	1.08	-20.37	Decrease
Sodium	Na	1.18	0.91	-29.67	Decrease
Sulphur	S	1.04	0.87	-19.54	Decrease
Magnesium	Mg	0.88	0.55	-60.00	Decrease
Chlorine	Cl	0.68	0.46	-47.83	Decrease
Oxygen	O	0.40	0.00	Disappeared	Disappeared
Titanium	Ti	0.14	0.00	Disappeared	Disappeared
Zinc	Zn	0.00	0.00	0.00	No Change
Spent Foundry Sand Modified Concrete @ 10 % Replacement					
Element	Symbol	*Without GA*	*With GA*	Diff (%)	Remarks
Calcium	Ca	68.77	54.74	-20.40	Decrease
Silver	Ag	2.80	3.73	33.21	Increase
Iron	Fe	3.14	11.89	278.66	Increase
Carbon	C	1.09	4.71	332.11	Increase
Potassium	K	1.53	5.54	262.09	Increase
Silicon	Si	11.38	9.27	-18.54	Decrease
Phosphorous	P	1.04	0.62	-40.38	Decrease
Aluminium	Al	3.57	3.68	3.08	Increase
Sodium	Na	0.31	1.10	254.84	Increase
Sulphur	S	1.41	1.15	-52.48	Decrease
Magnesium	Mg	0.23	0.31	34.78	Increase
Chlorine	Cl	1.09	1.31	20.18	Increase
Oxygen	O	0.58	1.94	234.48	Increase
Titanium	Ti	0.22	0.00	-100.00	Decrease
Zinc	Zn	2.84	0.00	-100.00	Decrease
Spent Foundry Sand-Gum Arabic Modified Concrete @ 20 % Replacement					
Element	Symbol	*Without GA*	*With GA*	Diff (%)	Remarks
Calcium	Ca	64.62	71.94	11.33	Increase
Silver	Ag	2.66	2.40	-9.77	Decrease
Iron	Fe	6.23	6.11	-1.93	Decrease
Carbon	C	1.38	1.01	-26.81	Decrease
Potassium	K	1.75	1.74	-0.57	Decrease
Silicon	Si	13.82	9.87	-28.58	Decrease
Potassium	P	1.04	0.86	-78.85	Decrease
Aluminum	Al	3.61	2.80	-22.44	Decrease
Sodium	Na	0.17	0.27	58.82	Increase
Sulphur	S	1.52	1.47	-3.29	Decrease
Magnesium	Mg	0.34	0.31	-8.82	Decrease
Chlorine	Cl	0.76	0.70	-7.89	Decrease
Oxygen	O	0.15	0.51	240.00	Increase
Titanium	Ti	0.00	0.00	0.00	No Change
Zinc	Zn	1.95	0.00	-100.00	Decrease

4.2. XRD and SEM Characteristics of SFS and GA

The XRD diffractograms of the SFS and GA are amorphous in nature, The SFS showed dominance of crystalline silica peaks which are mainly quartz (SiO_2) (Olson, 2024; Akhtar et al., 2023; Mavroulidou and Lawrence, 2019). The morphology of the SFS particle distributions showed that the shapes of the SFS are angular (Olson, 2024; Guney et al. 2010; Deng and Tikalsky, 2008; Javed et al., 1994). The length of the SFS is approximately 173.44 μm (Elinwa and Hazzard, 2017) as compared to 500 μm (Guney et al., 2010; Yazoghli-Marzouk et al., 2012; Desplanques et al., 2012) with diameter less than 2 μm (Javed et al., 1994; Desplanques et al., 2012; Renard et al., 2006). Mineral oxides with wt. % greater than 5 % are, C (45.18 %), Si (13.84 %), Fe (12.40 %), O (10.75 %), Al (9.40 %), Ta (5.42 %), and mineral oxides with wt. % less than 5 % are Pb (2.86 %), Ca (1.57 %), Mg (0.40 %). and Ti (0.14 %), respectively. The Ca/Si ratio is 0.11. Gum Arabic is a natural branched-chain multifunctional hydrocolloid with a highly neutral or slightly acidic, arabino-galactan-protein complex containing calcium, magnesium, and potassium (Desplanques et al., 2012). The Ca/Si is 1.85 and the mineral oxides with concentration ≥ 1.00 are C (59.61), O (25.64 %), B (4.40 %), Te (2.30 %), N (2.24 %), Ga (1.25 %), and Ca (1.07 %). Carbon (59.61 %) and Oxygen (25.64 %) are of substantial presence. These are Br (0.83 %), As (0.60 %), K (0.46 %), Si (0.41 %), Rb (0.35 %), P (0.31 %), Mg (0.31 %), and F (0.22 %). The Ca/Si is 2.61. GA consists mainly of high-molecular weight polysaccharides and their calcium, magnesium, and potassium salts, which on hydrolysis, yield three main fractions of polysaccharides and proteins, including arabinogalactan (AG), arabinogalactan protein (AGP), and glycoprotein (GP), which differ from their molecular weight and chemical composition (Desplanques et al., 2012).

4.3. Experimental Characterization of SFS-GA Concrete

The cube compressive strengths of the SFS and SFS-GA concrete are shown in Table 5 for both the SFS-concrete and SFS-GA concrete. It was observed for SFS-concrete that the design strength of 25 N/m^2 was achieved by M-10-S and M-20-S at ≥ 28 days of curing (Age), and M-30-S and M-40-S at ≥ 60 days of curing. The maximum strength of the concrete was at 10 % replacement of SFS by wt. % of fine aggregate. This optimum has been confirmed by other works using the same material (Elinwa and Hazzard, 2017). The SFS-GA mix exhibited the same performance of 10 % and 20 % at ≥ 28 days, and ≥ 60 days for 30 % and 40 % with maximum replacement at 10 %. Table 6 showed the percentage differences in the SFS and SFS-GA concrete. The reliability of the experimental data collected were confirmed using the Minitab 18 Software. This was to ascertain their adequacy. The statistical parameters examined the mean, standard deviation, variance and coefficient of variance (CV) measured for the Age, and *the Mix* for the SFS and SFS-GA concrete samples. The results of these exercises are shown in Table 7 and Table 8, and Table 9 and Table 10, respectively. The statistical mean, StDev, and CV for the SFS concrete specimens ranged from 17.42 – 34.45 N/m^2, 4.36 – 9.99 N/m^2, and 25.03 – 29.00 %, respectively, and for the SFS=GA concrete specimens the ranges are 17.45-30.48 N/m^2, 6.09-12.71 N/m^2 and 27.25-42.70 %, respectively. In several works as shown in (Müller and Rübner, 2006) the distribution of strength of test specimens was assumed to be Gaussian and thus could be described by the mean value and standard deviation. Findings of most researchers are that the standard deviation is independent on the concrete class (Müller and Rübner, 2006).

4.3.1. XRD Analysis of SFS and SFS-GA Concrete

The XRD spectrums of all SFS and SFS-GA samples cured for 28 days. showed that the samples are dominantly silica in the form of quartz (Elinwa, 2024). Table 11 is the crystalline phase, and height counts for samples at 100 % relative intensities (Elinwa, 2024). From Table 11 it is very clear of the impact of the GA admixture on the hydration products when SFS-concrete and SFS-GA concrete were compared. The effect of the addition of GA reduced the crystalline phase from ten (10) to approximately six (6) which is approximately forty (40) percent reduction. The peak heights at 100 % relative intensity were also reduced. The significance of this is confirmation of the role of GA as an emulsifier and a water reducer. Table 12 compared the control concrete with the SFS-concrete at the two replacement levels 0f 10 % and 20 %, respectively. It is observed that they contain the same mineral oxides (Hildebrandt, Quartz, Brownmillerite, Portlandite, Tricalcium aluminate) but with different wt. %. The values of the mineral oxides at 10 % replacement are a confirmation that 10 % is the optimum with maximum compressive strength. This assertion is further confirmed with the results in Table 13.

4.3.2. Microstructure of SFS and SFS-GA Concrete

The control concrete micrograph (Figure 1a) shows C-S-H gels with nodules and vast areas of somehow chalky gel dotted with unhydrated cement, calcium hydroxide and voids. The addition of GA-admixture improved the texture of the concrete showing a well distributed gel of C-S-H with reduced void sizes. Patches of aggregates and unhydrated cement observed on the micrograph of the control concrete disappeared due to the addition of GA-admixture (Fig.1b), confirming the dual function of GA-admixture. GA acts both as an emulsifier and an admixture. The 10 % SFS-modified concrete sample (Fig. 2a) showed remarkable transformations on the hydration products with a well distributed C-S-H gel, dotted portions of voids, and a well-developed texture. With modified-GA admixture, a more compact texture was achieved with C-S-H gel and other features noticed (Figure 2b). Figure 3a shows the micrograph of 20 % modified sample. It shows C-S-H gels with harsher textures and patches of SFS aggregate. This is because of the higher percentage of SFS replacement. The maximum replacement level of SFS for optimum hydration was at 10 % (Elinwa, 2014), and in this work. The excess of the 20 % SFS acts as filler material and thus, may justify the harsher texture of the microstructure. The GA modified 20 % SFS micrograph concrete sample is shown in Figure 3b. The microstructure showed a more uniform and well dispersed concrete with the formation of C-S-H gel and moderately formed nodules. GA-admixture helped to modify the harsh texture noticed with 20 % SFS concrete (Figure 3a), and reduced the pore sizes, thereby, given a more homogenous texture.

4.3.3. Structural Characteristics of SFS and SFS-GA concrete

Table 14 shows a comprehensive comparative analysis of the transformations that took place in the concrete samples as hydration proceeded. Fifteen (15) mineral oxides were dictated having different wt. %. These are believed to have impacted on the concrete characteristics such as strength etc. This table also compared the performances of the SFS-modified and SFS-GA modified concrete mix to assess the levels of impact by the various additives. This table showed how each mineral oxide was impacted as viewed by the oxides' difference columns. The 10 and 20 % SFS and their GA-modified concrete were compared with SFS as the control concrete. Table 15 on the other hand compared the performances of each additive on each mineral oxide within the same mix. For an objective comparison of the impact of these additives on the concrete characteristics the work considered weight concentrations that are 3 % and above as most impactful on the concrete samples. Based on this assumption, the dominant mineral oxides considering 10 and 20 % SFS-concrete samples as the control concrete for this exercise, and as the reference for comparison, the mineral oxides are Ca, Si, Ag, Fe, C, K and Al. The levels (wt. %) of impact by various mineral oxides in the concrete samples show that calcium (Ca) was very strong for all the concrete sample with wt. % $>$ 50 %. These mineral oxides may have played substantial roles in the modifications of the concrete characteristics and strength shown in Tables 5, 7-10. The presence of Ag mineral oxide in concrete have been associated with a change in the morphology of the pores for which some of which may be more elongated, and others may surround the sand grains (Aubert et al., 2004) and therefore, alter the paste-aggregate interface. It can also increase porosity by reacting with cement to form dihydrogen (Aubert et al., 2004; Murat and Sorrentino, 1996). Chromium in the parent material (SFS, Table 2b) has been associated with accelerating the setting time and modifying the quality of the hydrates formed (Maaouia, 2018; Macphee and Glasser, 1993; Spitz et al., 2018). Iron oxide is found in varying quantities in all the concrete samples. The Iron oxide layer is reported to improve the bond between cement and steel thereby contributing to good mechanical strength (Santamaría et al., 2017) and can lead to a degradation of the interfacial transition zone (ITZ) around some aggregates. Iron oxide can also reduce the amount of heat released during (Santamaría et al., 2017) hydration. The cumulative effects of these changes of porosity, hydration and paste-aggregate bonds of cementitious materials have been suggested could lead to changes in the mechanical properties of the concrete samples (Paul et al., 2021).

5. Conclusion

The mechanical strength and characteristics of SFS-admixed concrete have been investigated, and the following conclusions are drawn from the work:

i- The characteristics of spent foundry sand (SFS) confirmed that it has no cementing factor due to its fineness and thus required more water demand to achieve the requirements of concrete. For SFS to be used in concrete, the effects of its grading, surface properties and the binder proportions are very important for good concrete. Gum Arabic is an emulsifier acting as an admixture with low viscosity and high solubility. GA improved workability, compressive strength and reduced water to cement ratio (w/c). Spent foundry sand and gum Arabic are compatible and can be used together to produce good concrete. This was confirmed to influence the hydration products with remarkable transformations and well distributed C-S-H gel at the optimum replacement of 10 % SFS.

ii- The statistical analysis also confirmed the reliability of the experimental data that SFS and GA are compatible since the mechanical strength are dependent on many factors such as the cement, aggregates and the compaction level. The distribution of the strength of the test specimen was observed to be Gaussian and thus was able to be described by the mean values and standard deviation.

iii- The dominant mineral oxides are Ca, Si, Ag, Fe, C, K and Al with a very strong presence of Ca for concrete samples with SFS and GA. These mineral oxides may have played substantial role in the modification of the concrete samples.

6. References

A. M. Saleh (2001). To obtain high-strength concrete and the resistance through the improvement of natural additions. Ph.D. dissertation, International University of Civil Engineering, Moscow, Russia, 2001

Ahmad, J., Aslam, F., Zaid, O., Alyousef, R., & Alabduljabbar, H. (2021). Mechanical and durability characteristics of sustainable concrete modified with partial substitution of waste foundry sand. Structural Concrete, 22(5), 2775-2790.

Akhtar, M. N., Malkawi, D. A. H., Bani-Hani, K. A., & Malkawi, A. I. H. (2023). Durability assessment of sustainable mortar by incorporating the combination of solid wastes: an experimental study. Civil Engineering Journal, 9(11), 2770-2786.

Aubert, J. E., Husson, B., & Vaquier, A. (2004). Metallic aluminum in MSWI fly ash: quantification and influence on the properties of cement-based products. Waste Management, 24(6), 589-596.

Bilal, H.; Yaqub, M.; Rehman, S.K.U.; Abid, M.; Alyousef, R.; Alabduljabbar, H.; Aslam, F. Performance of Foundry Sand Concrete under Ambient and Elevated Temperatures. Materials 2019, 12, 2645. [CrossRef

Deng, A., & Tikalsky, P. J. (2008). Geotechnical and leaching properties of flowable fill incorporating waste foundry sand. Waste Management, 28(11), 2161-2170.

Desplanques, S., Renou, F., Grisel, M., & Malhiac, C. (2012). Impact of chemical composition of xanthan and acacia gums on the emulsification and stability of oil-in-water emulsions. Food Hydrocolloids, 27(2), 401-410.

Desplanques, S., Renou, F., Grisel, M., & Malhiac, C. (2012). Impact of chemical composition of xanthan and acacia gums on the emulsification and stability of oil-in-water emulsions. Food Hydrocolloids, 27(2), 401-410.

Elinwa A. U. (2022). Water absorption and density relations of gum Arabic-sawdust ash concrete. Int. Technology and Science Journal (ITSJ), 4, (1), 1-14.

Elinwa A. U. (2024). Spent Foundry Sand (SFS)-Gum Arabic Admixed Concrete: X-Ray Diffraction, Microstructure, Acid and Sulphate Analysis. International Journal of Research and Scientific Innovation (IJRSI), 11, (8), 1653-1683.

Elinwa, A. U. (2014). Spent Foundry Sand as Partial Replacement of Fine Aggregate in the Production of Concrete. IOSR Journal of Mechanical and Civil Engineering, 11(5), 76-82.

Elinwa, A. U. (2021). Mechanical strengths of sawdust-ash-admixed gum arabic concrete. Journal of Modern Materials, 8(1), 12-29.

Elinwa, A. U., & Hazzard, M. A. (2017). Effects of gum Arabic admixture on the mechanical strengths of cement paste and concrete. Advancements in Materials, 1, 25-39.

Elinwa, A. U., & Kabir, N. (2019). Flexural Strength and Compressive Strength Relations of Spent Foundry Sand Concrete. ACI Materials Journal, 116(6).

Elinwa, A. U., & Umar, M. (2017). X-ray diffraction and microstructure studies of gum Arabic-cement concrete. Construction and Building Materials, 156, 632-638.

Elinwa, A. U., Abdulbasir, G., & Abdulkadir, G. (2018). Gum Arabic as an admixture for cement concrete production. Construction and Building Materials, 176, 201-212.

Elinwa, A., Maibulangu, M., Ogbo, I., & Salisu, A. (2021). Density and Mechanical Strength of Gum Arabic-Sawdust Ash Concrete. Available at SSRN 3780727, 14 pp.

Guney, Y., Sari, Y. D., Yalcin, M., Tuncan, A., & Donmez, S. (2010). Re-usage of waste foundry sand in high-strength concrete. Waste Management, 30(8-9), 1705-1713.

Guney, Y., Sari, Y. D., Yalcin, M., Tuncan, A., & Donmez, S. (2010). Re-usage of waste foundry sand in high-strength concrete. Waste Management, 30(8-9), 1705-1713.

Javed, S., Lovell, C. W., & Wood, L. E. (1994). Waste foundry sand in asphalt concrete. Transportation research record, (1437), pp. 27–34.

Kumar, K. A., Rajasekhar, K., & Sashidhar, C. (2022). Experimental research on the effects of waste foundry sand on the strength and micro-structural properties of concrete. Civil Engineering Journal, 8(10), 2172-2189.

Maaouia, O. B. (2018). Aptitude des granulats issus des bétons de déconstruction à la réutilisation, vis-à-vis du CrVI: Impact des propriétés de la matrice cimentaire et identification des mécanismes de relargage (Doctoral dissertation, Université Paris-Est). (accessed on 15 October 2021).

Macphee, D. E., & Glasser, F. P. (1993). Immobilization science of cement systems. MRS bulletin, 18(3), 66-71.

Mavroulidou, M., & Lawrence, D. (2019). Can waste foundry sand fully replace structural concrete sand?. Journal of Material Cycles and Waste Management, 21, 594-605.

Mbugua, R., Salim, R., & Ndambuki, J. (2016). Effect of gum Arabic karroo as a water-reducing admixture in concrete. Materials, 9(2), 80.

Mohamed, A. M., Osman, M. H., Smaoui, H., & Mohd Ariffin, M. A. (2018). Durability and microstructure properties of concrete with arabic gum biopolymer admixture. Advances in Civil Engineering, 2018(1), 1962832.

Müller, U., & Rübner, K. (2006). The microstructure of concrete made with municipal waste incinerator bottom ash as an aggregate component. Cement and Concrete Research, 36(8), 1434-1443.

Murat, M., & Sorrentino, F. (1996). Effect of large additions of Cd, Pb, Cr, Zn, to cement raw meal on the composition and the properties of the clinker and the cement. Cement and concrete research, 26(3), 377-385.

Olson S. (2024). Engineering the future for sustainability measuring and communicating our progress. Proceedings Of A Forum, National Academies Press 500 Fifth Street, NW Washington, DC 20001

Paul, P., Belhaj, E., Diliberto, C., Apedo, K. L., & Feugeas, F. (2021). Comprehensive characterization of spent chemical foundry sand for use in concrete. Sustainability, 13(22), 12881.

Prasad, V. D., Prakash, E. L., Abishek, M., Dev, K. U., & Kiran, C. S. (2018). Study on concrete containing waste foundry sand, fly ash and polypropylene fibre using Taguchi method. Materials Today: Proceedings, 5(11), 23964-23973.

Prasad, V. D., Prakash, E. L., Abishek, M., Dev, K. U., & Kiran, C. S. (2018). Study on concrete containing waste foundry sand, fly ash and polypropylene fibre using Taguchi method. Materials Today: Proceedings, 5(11), 23964-23973.

Rashid, K., & Nazir, S. (2018). A sustainable approach to optimum utilization of used foundry sand in concrete. Science and Engineering of Composite Materials, 25(5), 927-937.

Raval A. D., Patel I. N., Pamnan A., & Kachwala A. I. (2015). Effect of Waste Foundry Sand as Partial Replacement of Sand in Concrete. Int.J. of Advance Engineering and Research Development, 2 (1), 19-22.

Renard, D., Lavenant-Gourgeon, L., Ralet, M. C., & Sanchez, C. (2006). Acacia s enegal gum: continuum of molecular species differing by their protein to sugar ratio, molecular weight, and charges. Biomacromolecules, 7(9), 2637-2649.

Santamaría, A., Orbe, A., Losañez, M. M., Skaf, M., Ortega-Lopez, V., & González, J. J. (2017). Self-compacting concrete incorporating electric arc-furnace steelmaking slag as aggregate. Materials & Design, 115, 179-193.

Siddique, R., Aggarwal, Y., Aggarwal, P., Kadri, E. H., & Bennacer, R. (2011). Strength, durability, and micro-structural properties of concrete made with used-foundry sand (UFS). Construction and Building Materials, 25(4), 1916-1925.

Siddique, R., De Schutter, G., & Noumowe, A. (2009). Effect of used-foundry sand on the mechanical properties of concrete. Construction and building materials, 23(2), 976-980.

Siddique, R., Kaur, G., & Rajor, A. (2010). Waste foundry sand and its leachate characteristics. Resources, Conservation and Recycling, 54(12), 1027-1036.

Spitz, N., Coniglio, N., El Mansori, M., Montagne, A., & Mezghani, S. (2018). Quantitative and representative adherence assessment of coated and uncoated concrete-formwork. Surface and Coatings technology, 352, 247-256.

Sugumaran, B., & Neme, I. (2024). Effect of adsorption interactions of Arabic gum with cement. Materials Research Express, 11(6), 065503.

Yazoghli-Marzouk, O., Vulcano-Greullet, N., Cantegrit, L., Friteyre, L., & Jullien, A. (2014). Recycling foundry sand in road construction–field assessment. Construction and Building Materials, 61, 69-78.